

DeNoising-MOT: Towards Multiple Object Tracking with Severe Occlusions

Teng Fu

Shanghai Key Laboratory of IIP
School of Computer Science,
Fudan University
Shanghai, China
fut21@m.fudan.edu.cn

Xiaocong Wang

Shanghai Key Laboratory of IIP
School of Computer Science,
Fudan University
Shanghai, China
xcwang20@fudan.edu.cn

Haiyang Yu

Shanghai Key Laboratory of IIP
School of Computer Science, Fudan
University
Shanghai, China
hyyu20@fudan.edu.cn

Ke Niu

Shanghai Key Laboratory of IIP
School of Computer Science,
Fudan University
Shanghai, China
kniu22@m.fudan.edu.cn

Bin Li

Shanghai Key Laboratory of IIP
School of Computer Science,
Fudan University
Shanghai, China
libin@fudan.edu.cn

Xiangyang Xue*

Shanghai Key Laboratory of IIP
School of Computer Science,
Fudan University
Shanghai, China
xyxue@fudan.edu.cn

ABSTRACT

Multiple object tracking (MOT) tends to become more challenging when severe occlusions occur. In this paper, we analyze the limitations of traditional Convolutional Neural Network-based methods and Transformer-based methods in handling occlusions and propose DN MOT, an end-to-end trainable DeNoising Transformer for MOT. To address the challenge of occlusions, we explicitly simulate the scenarios when occlusions occur. Specifically, we augment the trajectory with noises during training and make our model learn the denoising process in an encoder-decoder architecture, so that our model can exhibit strong robustness and perform well under crowded scenes. Additionally, we propose a Cascaded Mask strategy to better coordinate the interaction between different types of queries in the decoder to prevent the mutual suppression between neighboring trajectories under crowded scenes. Notably, the proposed method requires no additional modules like matching strategy and motion state estimation in inference. We conduct extensive experiments on the MOT17, MOT20, and DanceTrack datasets, and the experimental results show that our method outperforms previous state-of-the-art methods by a clear margin.

CCS CONCEPTS

• **Computing methodologies** → **Tracking; Motion capture.**

KEYWORDS

Multiple object tracking, Transformer, Occlusion handling, Set prediction.

*Corresponding author

Permission to make digital or hard copies of all or part of this work for personal or classroom use is granted without fee provided that copies are not made or distributed for profit or commercial advantage and that copies bear this notice and the full citation on the first page. Copyrights for components of this work owned by others than the author(s) must be honored. Abstracting with credit is permitted. To copy otherwise, or republish, to post on servers or to redistribute to lists, requires prior specific permission and/or a fee. Request permissions from [permissions@acm.org](https://www.acm.org/permissions).

MM '23, October 29–November 3, 2023, Ottawa, ON, Canada

© 2023 Copyright held by the owner/author(s). Publication rights licensed to ACM.

ACM ISBN 979-8-4007-0108-5/23/10...\$15.00

<https://doi.org/10.1145/3581783.3611728>

ACM Reference Format:

Teng Fu, Xiaocong Wang, Haiyang Yu, Ke Niu, Bin Li, and Xiangyang Xue. 2023. DeNoising-MOT: Towards Multiple Object Tracking with Severe Occlusions. In *Proceedings of the 31st ACM International Conference on Multimedia (MM '23)*, October 29–November 3, 2023, Ottawa, ON, Canada. ACM, New York, NY, USA, 19 pages. <https://doi.org/10.1145/3581783.3611728>

1 INTRODUCTION

Multiple Object Tracking (MOT) [6, 26, 93] is a fundamental computer vision task that involves predicting the trajectory of each object in a continuous image sequence while maintaining consistent object identity [5, 10, 33, 91]. In recent years, MOT has found wide application in areas such as autonomous driving and video surveillance. However, due to the complexity and crowdedness of real-world scenarios [2, 64], severe or even complete occlusions between objects are common. As a result, preventing ID switches under severe occlusions has become a critical challenge in MOT.

Recently, the Tracking-by-Detection (TBD) paradigm [6, 9, 44, 76, 97] has become the mainstream method for MOT due to its excellent efficiency and effectiveness. The paradigm benefits from the rapid development in the field of object detection and heavily relies on the detector's performance [28, 47, 49, 98]. However, when severe occlusion occurs, the object may become almost invisible in the 2D image, making it challenging to obtain the object's bounding box through the detection model. As shown in Figure 1(a), the middle person is occluded, and no detection result can be obtained, resulting in a failure to participate in the subsequent matching process. When the person reappears, a new trajectory is initiated.

Since the proposal of the Transformer [69] model in natural language processing, the attention model [68] has rapidly emerged in the field of computer vision [24, 39]. Following the success of the DETR methods [15, 35, 37, 67] in object detection, this structure has gradually been applied to multi-object tracking tasks. As illustrated in Figure 1(b), each existing trajectory will eventually receive a prediction result. However, due to occlusion-induced invisibility, these trajectories tend to predict lower confidence scores, leading to terrible results similar to those obtained in TBD methods.

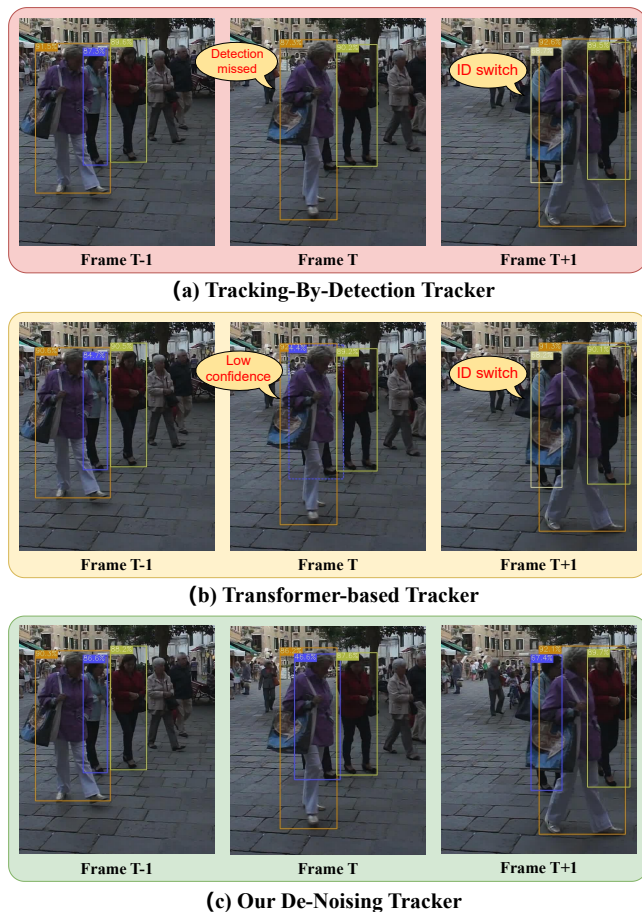


Figure 1: Visualization of a tracklet in the MOT17 dataset. Our model is robust to severe occlusions through Cascaded Mask Module and Denoising Training.

We further investigate the underlying mechanisms of the Transformer and observe that DETR [15] does not require Non-Maximum Suppression for post processing. Instead, it filters all outputs based on confidence and achieves excellent detection results. As illustrated in Figure 2, we can see that there is not always a one-to-one correspondence between the queries and the actual objects. Instead, multiple queries often attend to the same object. However, after the self-attention layers in the decoder, a query will suppress the neighboring queries. In the 2D-MOT task, due to the perspective relationship, objects are frequently subject to severe or even complete occlusion. This automatic suppression mechanism will also affect the queries responsible for two closely located objects. Ultimately, the confidence of the query responsible for the occluded object becomes lower, leading to the object being filtered out.

In this paper, we propose DeNoising MOT, abbreviated as DN-MOT, an online object tracker based on Transformer. Our fully end-to-end trainable model needs no additional module such as Kalman Filter [32] and Hungarian Matching [34] in inference. To improve the model’s ability to handle occlusions, we introduced Denoising Training and Cascaded Mask Module. As shown in Figure

1(c), our model exhibits better robustness against severe occlusions and maintains the tracking state of the object to prevent ID-Switch when it reappears.

The proposed method, based on DINO [88], first encodes the multi-scale features extracted by the CNN [30, 61]. And then, as in the previous methods [42, 87], we use track queries and detection queries to track existing trajectories and detect new trajectories, and introduce a Query Selection Module to give more reliable location prior for detection query. Subsequently, we create another type of queries, named denoising queries, to simulate the occurrence of occlusions. Specifically, we perform three types of noise to the locations of all objects in the ground truth based on whether there are other bounding box overlaps. The denoising queries are then fed into the decoder along with other queries to improve the model’s resistance to noise. Finally, to coordinate the interaction between different types of queries, we proposed a Cascaded Mask Module, which can help the queries in the decoder focus on their own trajectories and not be suppressed by neighboring trajectories. Importantly, the denoising query is not required in inference, and only two adjacent frames are needed as input in each time step, which significantly improves the time and space efficiency of our model.

The experimental results of DN-MOT on MOT Challenge [19, 43, 70] and DanceTrack [65] demonstrate that our model achieves the state-of-the-art performance among all end-to-end Transformer-based methods. These results highlight the importance of solving the occlusion problem, not only for enhancing application performance, but also for improving metrics such as MOTA and HOTA [7, 41]. Additional ablation experiments also illustrate the effectiveness of the proposed method.

2 RELATED WORK

In this section, we will provide a brief introduction to two paradigms commonly used in multi-object tracking, namely Tracking-By-Detection (TBD) methods and Transformer-based methods. We will also briefly explain how existing methods deal with the occlusion problem and their limitations.

2.1 Tracking-By-Detection Methods

Most multi-object tracking models based on convolutional neural networks adopt the Tracking-By-Detection (TBD) paradigm, which usually consists of two stages. Firstly, a detection model is used to detect objects in the frame, and then an association stage is performed on existing trajectories and detection results using motion information [58] or Re-ID information [75]. SORT [9] uses the Hungarian matching algorithm and Kalman filter to achieve these two processes, and Deep SORT [76] adds Re-ID features in the association stage. Subsequent models focus on improving association strategies [3, 18, 73], more robust action prediction [55, 81], and more efficient Re-ID feature extraction [51, 60, 84]. For example, ByteTrack [92] uses more detection results and a two-stage association process; OC SORT [14] iteratively updates the Kalman Filter through interpolation after the object reappears, while BoT-SORT [1] estimates the motion of the camera to correct the prediction of the Kalman filter. C-BIOU Tracker [83] uses buffered IOUs in the association process to increase the probability of successful

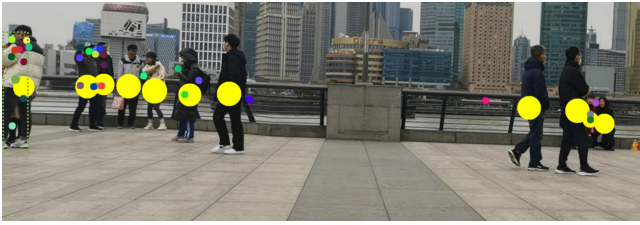


Figure 2: The reason that DETR-based models do not need NMS. We visualized all the queries whose prediction category is "person". We use yellow circles to represent the predictions that are not filtered out (the filtering threshold is 0.3), and use small circles of different colors to indicate results with low confidence.

association. However, these methods still struggle to handle False Negative objects.

2.2 Transformer-Based Methods

With the increasing popularity of the Transformer architecture in Natural Language Processing, this structure is now being widely used in Computer Vision tasks [24, 39, 85], and achieves comparable and even state-of-the-art results in some fields [17, 59, 71, 86]. In multi-object tracking, TransTrack [66] replaces the detection model and location prediction model in the TBD paradigm with a transformer architecture, while Trackformer [42] uses detection query and track query to detect new trajectories and track existing trajectories respectively. MeMOT [12] utilizes a memory buffer to enable the model to use both short-term and long-term information for better inference capabilities. These methods completely discard external modules such as the Kalman Filter used for location prediction in previous methods [16, 99] in inference. Moreover, with the recent advancements in multimodal models, some models also incorporate information from other modalities to enhance performance [20, 77, 100]. Our proposed DNMOT is also based on a fully end-to-end Transformer architecture and is equipped with a Denoising Training process and Cascaded Mask Module, which improves the model’s robustness to occlusions and leads to better performance on evaluation metrics.

2.3 Occlusion Handling

Severe occlusion usually leads to problems such as missed detections and ID switches, which seriously affect the performance of the model in crowded scenes. In recent years, researchers have started to address the issue of occlusion in multi-object tracking [80]. While using ReID information to match reappearing objects is a common method to handle occlusion [63], it does not work well for scenarios where the object is often locally invisible [13]. To address this issue, MotionTrack [46] uses the Interaction Module to model the relationship between tracks for better results in dense scenes; FineTrack [48] uses locally unoccluded parts for fine-grained feature extraction; P3AFormer [95] uses a point-wise approach to solve the occlusion problem at the pixel level; Some methods [44] also use calculation in the case of occlusion to determine whether the trajectory is terminated, rather than relying on inactivity time.

In contrast, our DNMOT uses a novel approach to simulate the occlusion occurrence by the noising method, enabling the model to learn the denoising process when occlusion occurs. This novel approach has shown to be highly effective in addressing the challenges associated with occlusion, and its effectiveness surpasses that of previous techniques. Our experiments show that this explicit treatment, which is completely different from previous methods, leads to better robustness of the model to occlusions.

3 METHODOLOGY

Given a sequence of video frames $I = \{I^0, I^1, \dots, I^t\}$, the proposed DNMOT model processes each frame sequentially and generates K trajectories $T = \{T_0, T_1, \dots, T_K\}$.

The pipeline of our method is illustrated in Figure 3. Our model consists of a Backbone that extracts multi-scale features and a Transformer structure that performs tracking. The extracted multi-scale features are flattened and concatenated before being encoded using self-attention in Transformer encoder. Then the encoded features are sent to the decoder as Key and Value, and a Query set containing Detection queries, Track queries, and Denoising queries is fed to the decoder simultaneously. After the cascaded mask decoder, these queries are used to initialize new trajectories, track active trajectories, and train the model to be robust to noises, respectively. We will explain how to generate the three types of queries in Section 3.2, while our network architecture and the Cascaded Mask Module it contains will be explained in Section 3.1 and Section 3.3, respectively.

3.1 Network Architecture

DNMOT consists of a backbone and an improved denoising Transformer architecture. In order to better integrate temporal information, we adopt multi-frame features. In this section, we will briefly introduce the details of our network architecture.

Backbone. We employ ResNet50 [30] as our feature extractor, utilizing the output of the last three layers of the model. We apply another convolution layer with a kernel size of 3 and a stride of 2 for the final layer’s output, and merge the features from the four scales to obtain the final feature vector $F \in \mathbb{R}^{B \times N_{\text{feature}} \times d}$. Here, N_{feature} represents the total number of features across the four scales, and d represents the dimension of the features.

Multi-frame Features. Following [74], we merge the backbone features of the current and previous frames and input them together into the Transformer structure. This enables the model to directly compare the object’s position between two frames. To provide the model with 3D position embeddings, including time, we use trigonometric functions as 2D position embeddings in ViT [24] and incorporate them into the Transformer [4, 8]. This helps the model to distinguish between two consecutive frames.

Transformer. Our main network architecture is based on the classic Transformer structure, which consists of an Encoder and a Decoder. The Encoder is made up of several consecutive layers, where each layer contains a multi-head self-attention module followed by a feed-forward network. Similarly, the Decoder also consists of several identical layers, and each layer includes a self-attention module, a cross-attention module, and a feed-forward network.

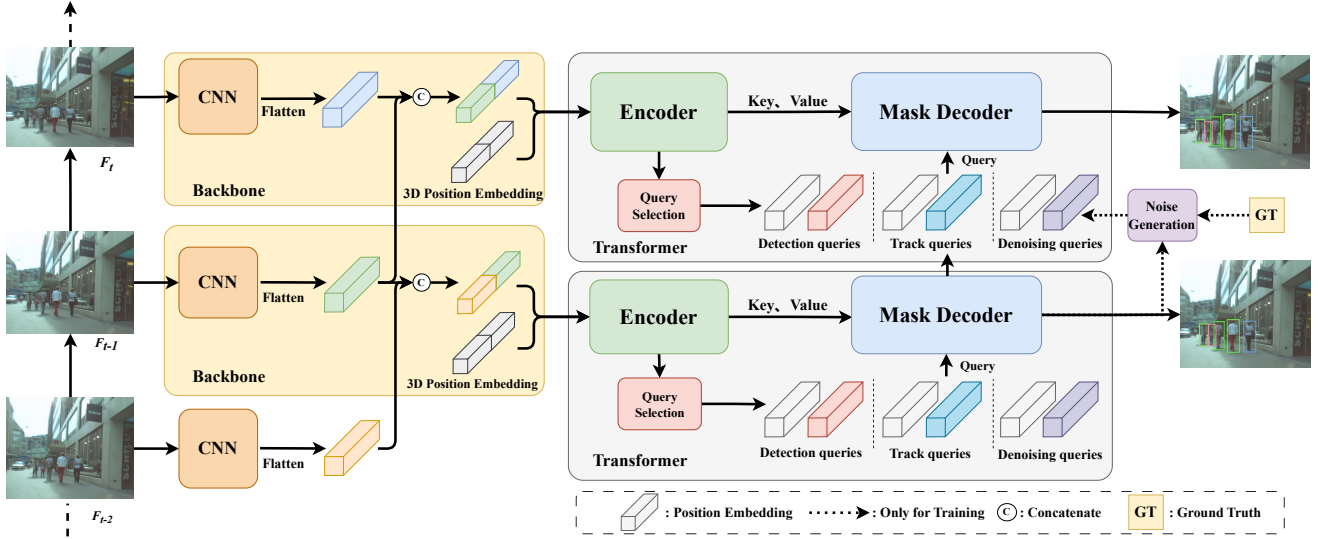


Figure 3: Overall architecture of the proposed method, consisting of a backbone for feature extraction and an Encoder-Decoder architecture. At each time step, the multi-scale features extracted from the input image will be flattened and concatenate with the features of the previous frame, and after the Encoder processing, the features will be selected to obtain the positions of interest. These positions will form detection queries with learnable embeddings, and then the track queries generated in the previous frame and the output of the Noise Generation module (Denoising queries) will be used as a Query set to pass into the Mask Decoder. Noise Generation will not be enabled during Inference.

3.2 Query Generation

The overall generation process is illustrated in Figure 4. Figure 4 (a) demonstrates how Query Selection is utilized to help the detection queries in more precisely locating the region of interest. Figure 4 (b) illustrates how the final denoising queries are generated via track queries and Ground Truths.

Detection Query. As illustrated in Figure 4(a), the detection query is responsible for detecting new trajectories. This query needs to address two main difficulties: (1) it must detect all objects in the frame [11, 29, 38]; (2) it must remove trajectories already activated in the detection results, as these trajectories are already represented by the track query. The detection queries are obtained by adding the content embedding and the position embedding. To help the queries find the region of interest faster, we use selected position embeddings instead of uniform position embeddings. Specifically, each output of encoder will generate a score by a MLP, which represents the probability of an object occurring at the location represented by the encoder output. The position embedding of the top N_d queries, where N_d is the number of detection queries and is typically set to 300, will be added with the same number of randomly initialized content queries to form the final detection query set. While we keep the learnable content queries to learn their own content embedding that helps to interact between different types of queries, we use the selected position embeddings to accelerate the detection process.

Track Query. Track query is used to continuously track all active trajectories, which are tracked and initialized in the previous

frame. Track queries from the previous frame that generates high-confidence track results are considered active trajectories, and their content embedding and position embedding in the current frame are obtained from the final layer’s output of the decoder and the generated object position, respectively. Additionally, new tracks with detection query results above the threshold λ_D in the previous frame are treated as new tracks and added to the track query of the current frame for subsequent tracking.

Denoising Query. The denoising query is utilized to simulate the scenario of occlusion. To achieve this, we create N groups of noise queries, where each group comprises the same number of positive noise as the objects present in the ground truth. Additionally, we generate an equal number of negative noise by utilizing a broader range of noise, inspired by the approach proposed in DINO [88]. Figure 4(b) depicts our generation process. Although our task involves only one category, we initially perturb the category numbers to a larger space with a uniform distribution, similar to DINO. The aim is not to differentiate between different categories. Instead, we adopt this method to yield a different mapping outcome for the category of pedestrians. This is because, in crowded scenes, occlusion tends to make pedestrians partially visible, thereby creating a significant difference between the acquired mapping vectors. Subsequently, we replace the embedding and the real object position with the existing content embedding and bounding box of the active trajectory. Finally, we employ various ranges of noise to perturb the position and map it to position embedding after perturbation. During the final loss calculation and back-propagation

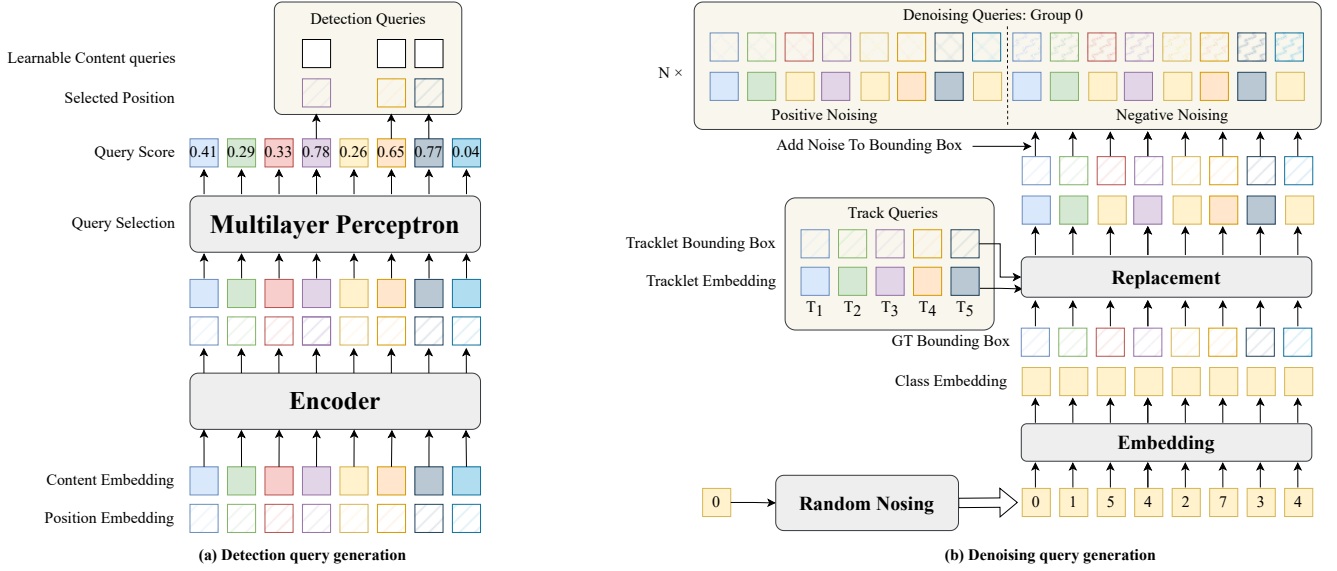


Figure 4: The generation process of queries in decoder. (a) illustrates how features extracted by backbone and encoder are filtered to provide location references for detection queries. (b) shows how to combine the existing active trajectories and ground truth information to generate the Denoising queries.

stage, we utilize the ground truth as supervision for positive noise and "no-object" as supervision information for negative noise.

We employ different strategies for generating positive noise depending on the presence of other objects around the object. A random noise vector $N = (n_x, n_y, n_w, n_h)$ is sampled, and all its elements are randomly chosen from a range between $-\lambda_r$ and λ_r for each of the four values of the bounding box $B = (x, y, w, h)$. The resulting coordinate information is obtained after the addition of the noise vector:

$$B_{\text{new}} = B + B \odot N \quad (1)$$

where \odot represents element-wise product. When an object is close to another object (with IOU greater than threshold τ_c), we introduce a conditional noise strategy, in which the final result is a weighted sum of the current object's bounding box and its neighboring object's bounding box:

$$B_{\text{new}} = \lambda_c B + (1 - \lambda_c) B_n \quad (2)$$

where B_n represents the bounding box of the neighboring object, and λ_c is a conditional noise factor between 0 and 1.

Figure 5 depicts our three noise addition methods. In (a), the bounding boxes of two neighboring objects are shown in green and yellow, respectively. (b), (c), and (d) demonstrate the results of positive random noising, positive conditional noising, and negative noising for the green object, respectively. Finally, the results of the three noise addition methods are merged to create a group of Denoising queries. The final Denoising query set comprises multiple groups of Denoising queries.

3.3 Cascaded Mask Self-attention

In the Decoder, the query undergoes two processes: self-attention and cross-attention. During self-attention, queries interact with

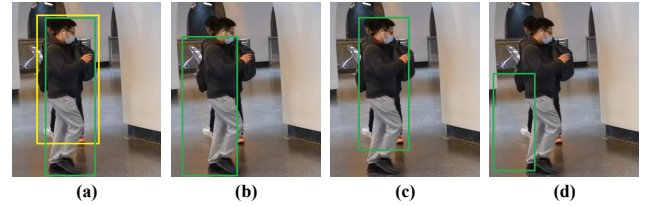


Figure 5: Visualization of different types of Noising. (a): ground truth of the object which we add noises to and its neighboring object. (b): with positive random noise. (c): with positive conditional noise. (d): with negative noise.

each other, potentially facilitating communication between queries carrying different information. In the subsequent cross-attention stage, the query interacts with all the keys and attends only to itself. All three types of queries require cross-attention to interact with features extracted earlier for fine-grained classification and regression tasks. However, the demands for the self-attention are different for each type of query.

For detection query, on the one hand, it needs to interact with other queries of the same type to ensure that no duplicate objects are detected. On the other hand, this type of query also needs to determine whether it is focusing on a new trajectory by interacting with the track queries.

For track query, self-attention may have suppressed effects on other queries in its vicinity. This mechanism is still needed for detection queries since their number is often larger than the actual number of new trajectories. However, in crowded scenes, trajectories often have tight spatial relationships with each other, and

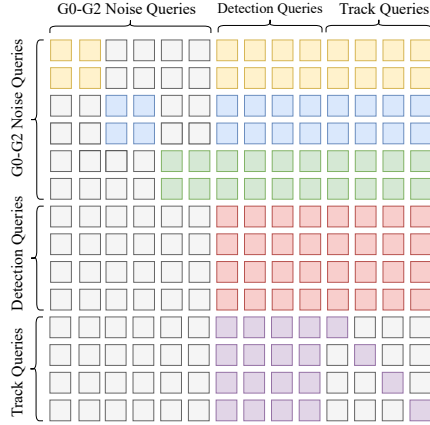


Figure 6: The cascaded mask used in the self-attention of the decoder layer. Different colors represent different types of queries or different groups of denoising queries. The gray parts indicate the invisibility between each other.

this mechanism often leads to the suppressed influence of occluded trajectory objects. On the other hand, the inter-relationship between trajectories, such as companions walking together, can help each other in the tracking process due to their similar speed and direction. Therefore, a mechanism that allows for interaction between trajectories without interfering with each other needs to be designed.

For Denoising query, it is a separate module. And it is important to ensure that different groups of denoising queries do not interfere with each other. This is because adding noise to different groups is a random process, and two groups of noise may potentially refer to each other. Therefore, it is necessary to ensure that any two groups of denoising queries are not visible to each other.

We have implemented the analysis mentioned above using the mask self-attention mechanism in our model. The mask is represented as a $N_q \times N_q$ matrix, where N_q is the number of queries. The i -th row corresponds to the invisibility mask for the i -th query in self-attention. The j -th location in this row is gray means that the j -th query is invisible to the i -th query during self-attention. It should be noted that we use a progressive visibility scheme for track queries. In the initial few layers, typically the first half of the decoder layers, the track queries are fully visible to each other, and each track query interacts with other queries to extract coupled information between them. In the subsequent layers, typically the latter half of the layers, as shown in Figure 6, we introduce masks to limit each track query’s interactions only with itself, thus preventing suppression by other queries.

3.4 Loss Function

Our model’s optimization is a bipartite matching problem, and we utilize set prediction loss, as in other transformer-based approaches [15].

Each track query corresponds to either a ground truth trajectory or a ‘no-object’ (which indicates the trajectory’s termination in the current frame). For detection queries, we use DETR’s bipartite

matching mechanism to establish the correspondence between the model outputs and the ground truths. Concerning denoising queries, we supervise positive and negative noises with actual ground truth and ‘no-object’ category, respectively. For classification score calculation, we employ focal loss [36], and for bounding box regression, we use L1 and IOU loss [50]. Our loss function is defined as:

$$\mathcal{L}_{\text{track}} = \lambda_{\text{focal}} \mathcal{L}_{\text{cls}} + \lambda_{\text{L1}} \mathcal{L}_{\text{bbox}} + \lambda_{\text{iou}} \mathcal{L}_{\text{iou}} \quad (3)$$

where λ_{focal} , λ_{L1} and λ_{iou} are the loss weights for balancing the focal loss, L1 loss and the IOU loss, respectively. In addition, similar to Deformable DETR [101], we add auxiliary losses after each decoder layer, and add extra intermediate losses after the query selection module, with the same components as for each decoder layer. Finally, our final loss function is defined as:

$$\mathcal{L} = \mathcal{L}_{\text{track}} + \mathcal{L}_{\text{aux}} + \mathcal{L}_{\text{inter}} \quad (4)$$

where $\mathcal{L}_{\text{track}}$ denotes the track loss in Equation 3, \mathcal{L}_{aux} denotes the auxiliary loss, and $\mathcal{L}_{\text{inter}}$ denotes the intermediate loss.

4 EXPERIMENTS

In this section, we demonstrate the performance of our model on three public datasets, namely MOT17 [43], MOT20 [19], and DanceTrack [65]. In addition, we conduct ablation experiments to verify the effectiveness of our modules.

4.1 Datasets and Metrics

Datasets. We evaluated our model’s performance on three publicly available datasets: MOT17 [43], MOT20 [19], and Dance Track [65] to ensure fair comparison. MOT17 consists of 7 training and 7 testing sequences, each with detection results from three existing detectors [27, 49, 82] for evaluating the association performance of methods. As our model is an end-to-end approach, we only conducted experiments on the private track. MOT20 includes 4 training and 4 testing sequences with more objects in the scene compared to MOT17. DanceTrack is a recent multi-object tracking dataset with 100 dance sequences, including 40 training sequences, 25 validation sequences, and 35 testing sequences.

Validation set. We conducted our ablation studies on MOT17. Due to the restrictions on the number of submissions for the test set in MOT Challenge [19, 43], we sampled half of each training sequence as our validation set followed by [93].

Metrics. We use CLEAR [7] MOT metrics and HOTA [41] as our evaluation metrics.

4.2 Implementation Details

We utilized PyTorch [45] to develop our model and carried out experiments on 8 NVIDIA 3090Ti GPUs. The image was resized to a minimum size of 800, and we employed data augmentation, such as random flipping and cropping.

Hyperparameters. Our model was pre-trained on Crowdhuman [57] for 80 epochs, followed by 40, 50, and 20 epochs of training on MOT17 [43], MOT20 [19], and DanceTrack [65], respectively. The initial learning rate was 2×10^{-4} and was decayed after the 10 epochs. We used the AdamW [40] optimizer. Our Transformer structure consisted of 6 encoder layers and 6 decoder layers, with 8 heads in the attention mechanism. After conducting ablation experiments, we set the number of detection queries to 300 and determined the

Table 1: Performance comparison between DNMOT and existing methods on the MOT17 dataset under the private detection protocols.

Method	MOTA \uparrow	IDF1 \uparrow	HOTA \uparrow	FP \downarrow	FN \downarrow	ID.Sw \downarrow
TraDeS [78]	69.1	63.9	52.7	20892	150060	3555
FairMOT [93]	73.7	72.3	59.3	27507	117477	3303
GTR [99]	75.3	71.5	59.1	26793	109854	2859
CorrTracker [72]	76.5	73.6	60.7	29808	99510	3396
OC-SORT [14]	78.0	77.5	63.2	15100	108000	1950
MOTRv2 [94]	78.6	75.0	62.0	23409	94797	2619
GHOST [56]	78.7	77.1	62.8	-	-	2325
ByteTrack [92]	80.3	77.3	63.1	25491	83721	2196
BoT-SORT [1]	80.6	79.5	64.6	22524	85398	1257
C-BIOU Tracker [83]	81.1	79.7	64.1	23136	82011	1455
TransCenter [80]	73.2	62.2	54.5	23112	123738	3663
TransTrack [66]	74.5	63.9	54.1	28323	112137	3663
MeMOT [12]	72.5	69.0	56.9	37221	115248	2724
MOTR [87]	73.4	68.6	57.8	-	-	2439
TrackFormer [42]	74.1	68.0	57.3	34602	108777	2829
DNMOT(Ours)	75.6	68.1	58.0	24960	110064	2529

number of denoising query groups based on the number of objects in the ground truth, with a total denoising quantity of no more than 200. The batch size was initially set to 2, but it was adjusted to 1 when using the multi-frame strategy due to memory limitations. We set λ_{focal} , λ_{L1} , and λ_{iou} to 1, 5, and 2, respectively.

4.3 Benchmark Results

In this section, we report the results of our experiments on three datasets: MOT17 [43], MOT20 [19], and DanceTrack [65]. Our experiments demonstrate that our method achieves state-of-the-art or comparable results under the MOTA and HOTA metrics among Transformer-based end-to-end multi-object trackers that do not rely on external detectors (e.g., YOLOX [28]). Trackers with gray background do not require additional modules for inference, and the best results among them are marked in bold.

MOT17. In Table 1, we present the results of our experiments on MOT17 [43]. Our DNMOT achieves the best performance among all methods that do not require additional modules for inference, with a MOTA of 75.6 and a HOTA of 58.0. It is worth mentioning that we only use the CrowdHuman [57] dataset for pre-training, without any other datasets [22, 23, 25, 79, 90, 96], yet we achieve comparable or even better results. Our model successfully tracks many invisible objects, with a low number of false positives and false negatives.

MOT20. We present our experimental results on the MOT20 dataset [19] in Table 2. Our DNMOT achieved 70.5 MOTA, 73.2 IDF1, and 58.6 HOTA, which are the best results among similar methods. Compared to MOT17, MOT20 has a more crowded distribution of objects, and our model’s high robustness to occlusion leads to a greater improvement on MOT20 (+1.9 in MOTA, +7.1 in IDF1 and +3.9 in HOTA) than on MOT17 (+1.5 in MOTA, -0.9 in IDF1 and +0.2 in HOTA).

DanceTrack. We conduct experiments on the recently proposed DanceTrack dataset [65], which focuses on evaluating the performance of the tracker association stage using the HOTA evaluation metric [41]. In Table 3, we present our results, which show that our

Table 2: Performance comparison between DNMOT and existing methods on the MOT20 dataset.

Method	MOTA \uparrow	IDF1 \uparrow	HOTA \uparrow	FP \downarrow	FN \downarrow	ID.Sw \downarrow
FairMOT [93]	61.8	67.3	54.6	103440	88901	5243
CorrTracker [72]	65.2	69.1	-	79429	95855	5183
OC-SORT [14]	75.5	75.9	62.1	18000	108000	913
ByteTrack [92]	77.8	75.2	61.3	26249	87594	1223
GHOST [56]	73.7	75.2	61.2	-	-	1264
BoT-SORT [1]	77.8	77.5	63.3	24638	88863	1257
TransTrack [66]	64.5	59.2	48.9	28566	151377	3565
TransCenter [80]	67.7	58.7	43.5	56435	107163	3759
MeMOT [12]	63.7	66.1	54.1	47882	137983	1938
TrackFormer [42]	68.6	65.7	54.7	20348	140373	1532
DNMOT(Ours)	70.5	73.2	58.6	29314	122252	987

Table 3: Performance comparison between DNMOT and existing methods on the DanceTrack test set.

Method	MOTA \uparrow	IDF1 \uparrow	HOTA \uparrow
OC-SORT [14]	75.5	75.9	62.1
TraDeS [78]	86.2	41.2	43.3
ByteTrack [92]	89.6	53.9	47.7
GHOST [56]	91.3	57.7	56.7
MOTRv2 [94]	92.1	76.0	73.4
MOTR [87]	79.7	54.2	51.5
DNMOT(Ours)	89.1	49.7	53.5

approach achieves a HOTA score of 53.5, outperforming comparable methods by 2.0 points. Furthermore, our approach achieves a MOTA score of 89.1 and an IDF1 score of 49.7.

4.4 Ablation Study

In this section, we conduct ablation experiments to demonstrate the effectiveness of our proposed method and discuss the model hyperparameters.

DNMOT Components. Table 4 shows the impact of integrating different components. The Baseline is Deformable DETR [101], and we add track query [42] to make baseline applicable to MOT tasks. Integrating our components into the baseline can gradually improve overall performance. The application of denoising queries gives the model stronger performance, improving MOTA by 3.8 and IDF1 by 5.6 over baseline, as well as reducing ID Switch by 77%. By adding multi-frame features, the model can learn the motion patterns of objects in two frames, further improving MOTA and IDF1 and reducing the number of ID switches. When using Query Selection Module, there are extra 0.4 and 0.6 improvements in MOTA and IDF1, respectively. Finally, after adding the cascaded mask, we obtain 75.4 MOTA, 71.0 IDF1 and 477 ID switches, which is a significant improvement over the original Baseline (5.1 MOTA, 8.0 IDF1 improvement and 87% ID switch reduction).

Noising Type. We evaluate the effects of three noise types and present the results in Table 5. The denoising part is removed as our baseline for ablation study. Adding positive random noises (second row in the table) improves the bounding box prediction results, resulting in a significant increase in MOTA(+2.6). The more accurate position output leads to better position embedding for the next frame’s track query, reducing the number of ID Switches.

Table 4: The effect of our contributions. Baseline is Deformable DETR with track queries added.

Method	MOTA↑	IDF1↑	ID.Sw↓
Baseline	70.3	63.0	3264
+Denoising query	74.1	68.6	774
+Multi-frame feature	74.4	69.5	699
+Query Selection	74.8	70.1	496
+Cascaded Mask	75.4	71.0	477

Table 5: The results of the experiments on different types of noise. We denote the different types of noise as follows: PRN: Positive Random Noises, NN: Negative Noises, PCN: Positive Conditional Noises.

PRN	NN	PCN	MOTA↑	IDF1↑	ID.Sw↓
			70.3	63.0	3264
✓			72.9	64.6	3636
✓	✓		73.2	65.8	1112
✓	✓	✓	74.1	68.6	774

The addition of negative noises (third row in the table) resulted in the rejection of proposals that are farther away, further improving MOTA (+0.3) and IDF1 (+1.2) while reducing the number of ID switches. The introduction of positive conditional noises results in the best performance on the validation set, achieving 74.1 MOTA, 68.6 IDF1, and 774 ID switch numbers.

Cascaded Mask. We conduct experiments to demonstrate the effectiveness of our mask module and present our experimental results in Table 6. We use Trackformer [42] as our baseline and conducted ablation experiments on it (first row in the table). We modify the self-attention part in the decoder while keeping other parameters constant. We try three modifications: processing track queries separately using an MLP (second row in the table), adding a mask to all decoder layers for track queries (third row in the table), and gradually adding a mask to track queries using a cascaded approach (fourth row in the table).

We use an MLP with only linear and ReLU layers to process the track queries. However, our experiment shows a slight drop in performance when using an MLP to process the track queries separately. We believe this is due to two reasons. First, there are logical relationships between track queries that can aid in easier tracking by linking them together. The use of an MLP breaks this connection. Second, using attention and MLP to process two types of queries separately may not result in the same feature space, making it challenging for subsequent cross-attention and thus affecting the model’s optimization.

We further utilize the mask mechanism to ensure that the outputs of all query self-attention belong to the same feature space. However, using masks for all track queries throughout the decoder results in a decrease in metrics, suggesting that the interaction between tracks is still meaningful. To address this issue, we adopt a gradually added mask mechanism where masks are not added to track queries in the early decoder layers, allowing track queries to interact with each other. In later layers, masks are added so that

Table 6: Experimental results with different mask methods.

Method	MOTA↑	IDF1↑	ID.Sw↓
Baseline [42]	74.2	71.8	1449
MLP	74.1	71.5	1533
Full Mask	69.4	60.2	1086
Cascaded Mask	74.5	68.6	838

Table 7: The experimental results of choosing the hyperparameter λ_d and λ_t .

λ_d	λ_t	MOTA↑	IDF1↑	ID.Sw↓
0.4	0.3	73.9	66.7	1005
0.4	0.4	73.6	66.6	1042
0.4	0.5	72.8	66.1	1167
0.3	0.4	73.7	65.9	1298
0.4	0.4	73.6	66.6	1042
0.5	0.4	72.9	66.5	863

track queries could focus on their own objects without interference. Our experiments demonstrate that this Cascaded Mask module is highly effective and helps our model achieve the best results.

Threshold Selection. We investigate the impact of different threshold choices for different queries on the final results. The experimental results are shown in Table 7. For track queries, the best performance in terms of MOTA and IDF1 is achieved with a value of 0.3 for parameter λ_t . Conversely, for detection queries, the performance of the model is not sensitive to changes in parameter λ_d .

4.5 Discussion

In terms of IOU scores between objects, MOT17 is not heavily crowded and MOT20 is more crowded. However, in MOT20, sequences are often shot from a top-down perspective, and although people are close to each other, they do not obstruct each other. Therefore, compared to improvements in MOTA and HOTA, our method has greater value in application.

5 CONCLUSION

In this work, we propose DNMOT, an end-to-end trainable multi-object tracker based on the Transformer architecture. DNMOT adds noises during training and learns to denoising, resulting in stronger robustness in severe occluded scenes. Our method achieves state-of-the-art performance among all methods that do not require any additional modules during inference.

We hope those methods will foster future work for multi-object tracking with severe occlusions.

ACKNOWLEDGEMENTS

This work was supported in part by the National Natural Science Foundation of China (No.62176060), STCSM project (No.22511105000), Shanghai Municipal Science and Technology Major Project (No.2021SHZDZX0103), and the Program for Professor of Special Appointment (Eastern Scholar) at Shanghai Institutions of Higher Learning.

REFERENCES

- [1] Nir Aharon, Roy Orfaig, and Ben-Zion Bobrovsky. 2022. BoT-SORT: Robust associations multi-pedestrian tracking. *arXiv preprint arXiv:2206.14651* (2022).
- [2] Alexandre Alahi, Kratarth Goel, Vignesh Ramanathan, Alexandre Robicquet, Li Fei-Fei, and Silvio Savarese. 2016. Social lstm: Human trajectory prediction in crowded spaces. In *Proceedings of the IEEE conference on computer vision and pattern recognition*. 961–971.
- [3] Anton Andriyenko and Konrad Schindler. 2011. Multi-target tracking by continuous energy minimization. In *CVPR 2011*. IEEE, 1265–1272.
- [4] Anurag Arnab, Mostafa Dehghani, Georg Heigold, Chen Sun, Mario Lučić, and Cordelia Schmid. 2021. Vivit: A video vision transformer. In *Proceedings of the IEEE/CVF international conference on computer vision*. 6836–6846.
- [5] Jerome Berclaz, Francois Fleuret, Engin Turetken, and Pascal Fua. 2011. Multiple object tracking using k-shortest paths optimization. *IEEE transactions on pattern analysis and machine intelligence* 33, 9 (2011), 1806–1819.
- [6] Philipp Bergmann, Tim Meinhardt, and Laura Leal-Taixe. 2019. Tracking without bells and whistles. In *Proceedings of the IEEE/CVF International Conference on Computer Vision*. 941–951.
- [7] Keni Bernardin and Rainer Stiefelhagen. 2008. Evaluating multiple object tracking performance: the clear mot metrics. *EURASIP Journal on Image and Video Processing* 2008 (2008), 1–10.
- [8] Gedas Bertasius, Heng Wang, and Lorenzo Torresani. 2021. Is space-time attention all you need for video understanding?. In *ICML*, Vol. 2. 4.
- [9] Alex Bewley, Zongyuan Ge, Lionel Ott, Fabio Ramos, and Ben Upcroft. 2016. Simple online and realtime tracking. In *2016 IEEE international conference on image processing (ICIP)*. IEEE, 3464–3468.
- [10] Erik Bochinski, Volker Eiselein, and Thomas Sikora. 2017. High-speed tracking-by-detection without using image information. In *2017 14th IEEE international conference on advanced video and signal based surveillance (AVSS)*. IEEE, 1–6.
- [11] Alexey Bochkovskiy, Chien-Yao Wang, and Hong-Yuan Mark Liao. 2020. Yolov4: Optimal speed and accuracy of object detection. *arXiv preprint arXiv:2004.10934* (2020).
- [12] Jiarui Cai, Mingze Xu, Wei Li, Yuanjun Xiong, Wei Xia, Zhuowen Tu, and Stefano Soatto. 2022. MeMOT: multi-object tracking with memory. In *Proceedings of the IEEE/CVF Conference on Computer Vision and Pattern Recognition*. 8090–8100.
- [13] Jinkun Cao, Jiangmiao Pang, Xinhua Weng, Rawal Khirodkar, and Kris M Kitani. [n. d.]. Object Tracking by Hierarchical Part-Whole Attention. ([n. d.]).
- [14] Jinkun Cao, Xinhua Weng, Rawal Khirodkar, Jiangmiao Pang, and Kris Kitani. 2022. Observation-centric sort: Rethinking sort for robust multi-object tracking. *arXiv preprint arXiv:2203.14360* (2022).
- [15] Nicolas Carion, Francisco Massa, Gabriel Synnaeve, Nicolas Usunier, Alexander Kirillov, and Sergey Zagoruyko. 2020. End-to-end object detection with transformers. In *Computer Vision—ECCV 2020: 16th European Conference, Glasgow, UK, August 23–28, 2020, Proceedings, Part 1* 16. Springer, 213–229.
- [16] Mingfei Chen, Yue Liao, Si Liu, Fei Wang, and Jenq-Neng Hwang. 2022. TR-MOT: Multi-Object Tracking by Reference. *arXiv preprint arXiv:2203.16621* (2022).
- [17] Peng Chu, Jiang Wang, Quanzeng You, Haibin Ling, and Zicheng Liu. 2023. Transmot: Spatial-temporal graph transformer for multiple object tracking. In *Proceedings of the IEEE/CVF Winter Conference on Applications of Computer Vision*. 4870–4880.
- [18] Peng Dai, Renliang Weng, Wongun Choi, Changshui Zhang, Zhangping He, and Wei Ding. 2021. Learning a proposal classifier for multiple object tracking. In *Proceedings of the IEEE/CVF Conference on Computer Vision and Pattern Recognition*. 2443–2452.
- [19] Patrick Dendorfer, Hamid Rezatofighi, Anton Milan, Javen Shi, Daniel Cremers, Ian Reid, Stefan Roth, Konrad Schindler, and Laura Leal-Taixé. 2020. Mot20: A benchmark for multi object tracking in crowded scenes. *arXiv preprint arXiv:2003.09003* (2020).
- [20] Patrick Dendorfer, Vladimir Yugay, Aljosa Osep, and Laura Leal-Taixé. 2022. Quo Vadis: Is Trajectory Forecasting the Key Towards Long-Term Multi-Object Tracking? *Advances in Neural Information Processing Systems* 35 (2022), 15657–15671.
- [21] Prafulla Dhariwal and Alexander Nichol. 2021. Diffusion models beat gans on image synthesis. *Advances in Neural Information Processing Systems* 34 (2021), 8780–8794.
- [22] Piotr Dollár, Christian Wojek, Bernt Schiele, and Pietro Perona. 2009. Pedestrian detection: A benchmark. In *2009 IEEE conference on computer vision and pattern recognition*. IEEE, 304–311.
- [23] Piotr Dollár, Christian Wojek, Bernt Schiele, and Pietro Perona. 2011. Pedestrian detection: An evaluation of the state of the art. *IEEE transactions on pattern analysis and machine intelligence* 34, 4 (2011), 743–761.
- [24] Alexey Dosovitskiy, Lucas Beyer, Alexander Kolesnikov, Dirk Weissenborn, Xiaohua Zhai, Thomas Unterthiner, Mostafa Dehghani, Matthias Minderer, Georg Heigold, Sylvain Gelly, et al. 2020. An image is worth 16x16 words: Transformers for image recognition at scale. *arXiv preprint arXiv:2010.11929* (2020).
- [25] Andreas Ess, Bastian Leibe, Konrad Schindler, and Luc Van Gool. 2008. A mobile vision system for robust multi-person tracking. In *2008 IEEE Conference on Computer Vision and Pattern Recognition*. IEEE, 1–8.
- [26] Christoph Feichtenhofer, Axel Pinz, and Andrew Zisserman. 2017. Detect to track and track to detect. In *Proceedings of the IEEE international conference on computer vision*. 3038–3046.
- [27] Pedro F Felzenszwalb, Ross B Girshick, David McAllester, and Deva Ramanan. 2009. Object detection with discriminatively trained part-based models. *IEEE transactions on pattern analysis and machine intelligence* 32, 9 (2009), 1627–1645.
- [28] Zheng Ge, Songtao Liu, Feng Wang, Zeming Li, and Jian Sun. 2021. Yolox: Exceeding yolo series in 2021. *arXiv preprint arXiv:2107.08430* (2021).
- [29] Kaiming He, Georgia Gkioxari, Piotr Dollár, and Ross Girshick. 2017. Mask r-cnn. In *Proceedings of the IEEE international conference on computer vision*. 2961–2969.
- [30] Kaiming He, Xiangyu Zhang, Shaoqing Ren, and Jian Sun. 2016. Deep residual learning for image recognition. In *Proceedings of the IEEE conference on computer vision and pattern recognition*. 770–778.
- [31] Jonathan Ho, Ajay Jain, and Pieter Abbeel. 2020. Denoising diffusion probabilistic models. *Advances in Neural Information Processing Systems* 33 (2020), 6840–6851.
- [32] Rudolph Emil Kalman. 1960. A new approach to linear filtering and prediction problems. (1960).
- [33] Chanh Kim, Fuxin Li, Arridhana Ciptadi, and James M Rehg. 2015. Multiple hypothesis tracking revisited. In *Proceedings of the IEEE international conference on computer vision*. 4696–4704.
- [34] Harold W Kuhn. 1955. The Hungarian method for the assignment problem. *Naval research logistics quarterly* 2, 1-2 (1955), 83–97.
- [35] Feng Li, Hao Zhang, Shilong Liu, Jian Guo, Lionel M Ni, and Lei Zhang. 2022. Dn-detr: Accelerate detr training by introducing query denoising. In *Proceedings of the IEEE/CVF Conference on Computer Vision and Pattern Recognition*. 13619–13627.
- [36] Tsung-Yi Lin, Priya Goyal, Ross Girshick, Kaiming He, and Piotr Dollár. 2017. Focal loss for dense object detection. In *Proceedings of the IEEE international conference on computer vision*. 2980–2988.
- [37] Shilong Liu, Feng Li, Hao Zhang, Xiao Yang, Xianbiao Qi, Hang Su, Jun Zhu, and Lei Zhang. 2022. Dab-detr: Dynamic anchor boxes are better queries for detr. *arXiv preprint arXiv:2201.12329* (2022).
- [38] Wei Liu, Dragomir Anguelov, Dumitru Erhan, Christian Szegedy, Scott Reed, Cheng-Yang Fu, and Alexander C Berg. 2016. Ssd: Single shot multibox detector. In *Computer Vision—ECCV 2016: 14th European Conference, Amsterdam, The Netherlands, October 11–14, 2016, Proceedings, Part 1* 14. Springer, 21–37.
- [39] Ze Liu, Yutong Lin, Yue Cao, Han Hu, Yixuan Wei, Zheng Zhang, Stephen Lin, and Baining Guo. 2021. Swin transformer: Hierarchical vision transformer using shifted windows. In *Proceedings of the IEEE/CVF international conference on computer vision*. 10012–10022.
- [40] Ilya Loshchilov and Frank Hutter. 2017. Decoupled weight decay regularization. *arXiv preprint arXiv:1711.05101* (2017).
- [41] Jonathon Luiten, Aljosa Osep, Patrick Dendorfer, Philip Torr, Andreas Geiger, Laura Leal-Taixé, and Bastian Leibe. 2021. Hota: A higher order metric for evaluating multi-object tracking. *International journal of computer vision* 129 (2021), 548–578.
- [42] Tim Meinhardt, Alexander Kirillov, Laura Leal-Taixe, and Christoph Feichtenhofer. 2022. Trackformer: Multi-object tracking with transformers. In *Proceedings of the IEEE/CVF conference on computer vision and pattern recognition*. 8844–8854.
- [43] Anton Milan, Laura Leal-Taixé, Ian Reid, Stefan Roth, and Konrad Schindler. 2016. MOT16: A benchmark for multi-object tracking. *arXiv preprint arXiv:1603.00831* (2016).
- [44] Mohammad Hossein Nasser, Mohammadreza Babae, Hadi Moradi, and Reshad Hosseini. 2023. Online relational tracking with camera motion suppression. *Journal of Visual Communication and Image Representation* 90 (2023), 103750.
- [45] Adam Paszke, Sam Gross, Francisco Massa, Adam Lerer, James Bradbury, Gregory Chanan, Trevor Killeen, Zeming Lin, Natalia Gimelshein, Luca Antiga, et al. 2019. Pytorch: An imperative style, high-performance deep learning library. *Advances in neural information processing systems* 32 (2019).
- [46] Zheng Qin, Sanping Zhou, Le Wang, Jinghai Duan, Gang Hua, and Wei Tang. 2023. MotionTrack: Learning Robust Short-term and Long-term Motions for Multi-Object Tracking. *arXiv preprint arXiv:2303.10404* (2023).
- [47] Joseph Redmon, Santosh Divvala, Ross Girshick, and Ali Farhadi. 2016. You only look once: Unified, real-time object detection. In *Proceedings of the IEEE conference on computer vision and pattern recognition*. 779–788.
- [48] Hao Ren, Shoudong Han, Huilin Ding, Ziwen Zhang, Hongwei Wang, and Faquan Wang. 2023. Focus On Details: Online Multi-object Tracking with Diverse Fine-grained Representation. *arXiv preprint arXiv:2302.14589* (2023).
- [49] Shaoqing Ren, Kaiming He, Ross Girshick, and Jian Sun. 2015. Faster r-cnn: Towards real-time object detection with region proposal networks. *Advances in neural information processing systems* 28 (2015).
- [50] Hamid Rezatofighi, Nathan Tsoi, JunYoung Gwak, Amir Sadeghian, Ian Reid, and Silvio Savarese. 2019. Generalized intersection over union: A metric and a loss for bounding box regression. In *Proceedings of the IEEE/CVF conference on*

- computer vision and pattern recognition*. 658–666.
- [51] Ergys Ristani and Carlo Tomasi. 2018. Features for multi-target multi-camera tracking and re-identification. In *Proceedings of the IEEE conference on computer vision and pattern recognition*. 6036–6046.
 - [52] Robin Rombach, Andreas Blattmann, Dominik Lorenz, Patrick Esser, and Björn Ommer. 2022. High-resolution image synthesis with latent diffusion models. In *Proceedings of the IEEE/CVF Conference on Computer Vision and Pattern Recognition*. 10684–10695.
 - [53] Nataniel Ruiz, Yuanzhen Li, Varun Jampani, Yael Pritch, Michael Rubinstein, and Kfir Aberman. 2022. Dreambooth: Fine tuning text-to-image diffusion models for subject-driven generation. *arXiv preprint arXiv:2208.12242* (2022).
 - [54] Chitwan Saharia, William Chan, Saurabh Saxena, Lala Li, Jay Whang, Emily L Denton, Kamyar Ghasemipour, Raphael Gontijo Lopes, Burcu Karagol Ayan, Tim Salimans, et al. 2022. Photorealistic text-to-image diffusion models with deep language understanding. *Advances in Neural Information Processing Systems* 35 (2022), 36479–36494.
 - [55] Fatemeh Saleh, Sadegh Aliakbarian, Hamid Rezaatofghi, Mathieu Salzmann, and Stephen Gould. 2021. Probabilistic tracklet scoring and inpainting for multiple object tracking. In *Proceedings of the IEEE/CVF Conference on Computer Vision and Pattern Recognition*. 14329–14339.
 - [56] Jenny Seidenschwarz, Guillem Braso, Ismail Elezi, and Laura Leal-Taixé. 2022. Simple Cues Lead to a Strong Multi-Object Tracker. *arXiv preprint arXiv:2206.04656* (2022).
 - [57] Shuai Shao, Zijian Zhao, Boxun Li, Tete Xiao, Gang Yu, Xiangyu Zhang, and Jian Sun. 2018. Crowdhuman: A benchmark for detecting human in a crowd. *arXiv preprint arXiv:1805.00123* (2018).
 - [58] Sarthak Sharma, Junaid Ahmed Ansari, J Krishna Murthy, and K Madhava Krishna. 2018. Beyond pixels: Leveraging geometry and shape cues for online multi-object tracking. In *2018 IEEE International Conference on Robotics and Automation (ICRA)*. IEEE, 3508–3515.
 - [59] Baoguang Shi, Xiang Bai, and Cong Yao. 2016. An end-to-end trainable neural network for image-based sequence recognition and its application to scene text recognition. *IEEE transactions on pattern analysis and machine intelligence* 39, 11 (2016), 2298–2304.
 - [60] Bing Shuai, Andrew Berneshaw, Xinyu Li, Davide Modolo, and Joseph Tighe. 2021. Siammot: Siamese multi-object tracking. In *Proceedings of the IEEE/CVF conference on computer vision and pattern recognition*. 12372–12382.
 - [61] Karen Simonyan and Andrew Zisserman. 2014. Very deep convolutional networks for large-scale image recognition. *arXiv preprint arXiv:1409.1556* (2014).
 - [62] Jiaming Song, Chenlin Meng, and Stefano Ermon. 2020. Denoising diffusion implicit models. *arXiv preprint arXiv:2010.02502* (2020).
 - [63] Daniel Stadler and Jurgen Beyerer. 2021. Improving multiple pedestrian tracking by track management and occlusion handling. In *Proceedings of the IEEE/CVF conference on computer vision and pattern recognition*. 10958–10967.
 - [64] Russell Stewart, Mykhaylo Andriuk, and Andrew Y Ng. 2016. End-to-end people detection in crowded scenes. In *Proceedings of the IEEE conference on computer vision and pattern recognition*. 2325–2333.
 - [65] Peize Sun, Jinkun Cao, Yi Jiang, Zehuan Yuan, Song Bai, Kris Kitani, and Ping Luo. 2022. Dancetrack: Multi-object tracking in uniform appearance and diverse motion. In *Proceedings of the IEEE/CVF Conference on Computer Vision and Pattern Recognition*. 20993–21002.
 - [66] Peize Sun, Jinkun Cao, Yi Jiang, Rufeng Zhang, Enze Xie, Zehuan Yuan, Changhu Wang, and Ping Luo. 2020. Transtrack: Multiple object tracking with transformer. *arXiv preprint arXiv:2012.15460* (2020).
 - [67] Peize Sun, Rufeng Zhang, Yi Jiang, Tao Kong, Chenfeng Xu, Wei Zhan, Masayoshi Tomizuka, Lei Li, Zehuan Yuan, Changhu Wang, et al. 2021. Sparse r-cnn: End-to-end object detection with learnable proposals. In *Proceedings of the IEEE/CVF conference on computer vision and pattern recognition*. 14454–14463.
 - [68] Ilya Sutskever, Oriol Vinyals, and Quoc V Le. 2014. Sequence to sequence learning with neural networks. *Advances in neural information processing systems* 27 (2014).
 - [69] Ashish Vaswani, Noam Shazeer, Niki Parmar, Jakob Uszkoreit, Llion Jones, Aidan N Gomez, Łukasz Kaiser, and Illia Polosukhin. 2017. Attention is all you need. *Advances in neural information processing systems* 30 (2017).
 - [70] Paul Voigtlaender, Michael Krause, Aljosa Osep, Jonathon Luiten, Berin Balchandar Gnana Sekar, Andreas Geiger, and Bastian Leibe. 2019. Mots: Multi-object tracking and segmentation. In *Proceedings of the IEEE/CVF conference on computer vision and pattern recognition*. 7942–7951.
 - [71] Junke Wang, Dongdong Chen, Zuxuan Wu, Chong Luo, Xiyang Dai, Lu Yuan, and Yu-Gang Jiang. 2023. OmniTracker: Unifying Object Tracking by Tracking-with-Detection. *arXiv preprint arXiv:2303.12079* (2023).
 - [72] Qiang Wang, Yun Zheng, Pan Pan, and Yinghui Xu. 2021. Multiple object tracking with correlation learning. In *Proceedings of the IEEE/CVF Conference on Computer Vision and Pattern Recognition*. 3876–3886.
 - [73] Yongxin Wang, Kris Kitani, and Xinshuo Weng. 2021. Joint object detection and multi-object tracking with graph neural networks. In *2021 IEEE International Conference on Robotics and Automation (ICRA)*. IEEE, 13708–13715.
 - [74] Yuqing Wang, Zhaoliang Xu, Xinlong Wang, Chunhua Shen, Baoshan Cheng, Hao Shen, and Huaxia Xia. 2021. End-to-end video instance segmentation with transformers. In *Proceedings of the IEEE/CVF conference on computer vision and pattern recognition*. 8741–8750.
 - [75] Zhongdao Wang, Liang Zheng, Yixuan Liu, Yali Li, and Shengjin Wang. 2020. Towards real-time multi-object tracking. In *Computer Vision—ECCV 2020: 16th European Conference, Glasgow, UK, August 23–28, 2020, Proceedings, Part XI* 16. Springer, 107–122.
 - [76] Nicolai Wojke, Alex Bewley, and Dietrich Paulus. 2017. Simple online and realtime tracking with a deep association metric. In *2017 IEEE international conference on image processing (ICIP)*. IEEE, 3645–3649.
 - [77] Dongming Wu, Wencheng Han, Tiancai Wang, Xingping Dong, Xiangyu Zhang, and Jianbing Shen. 2023. Referring Multi-Object Tracking. *arXiv preprint arXiv:2303.03366* (2023).
 - [78] Jialian Wu, Jiale Cao, Liangchen Song, Yu Wang, Ming Yang, and Junsong Yuan. 2021. Track to detect and segment: An online multi-object tracker. In *Proceedings of the IEEE/CVF conference on computer vision and pattern recognition*. 12352–12361.
 - [79] Tong Xiao, Shuang Li, Bocho Wang, Liang Lin, and Xiaogang Wang. 2017. Joint detection and identification feature learning for person search. In *Proceedings of the IEEE conference on computer vision and pattern recognition*. 3415–3424.
 - [80] Yihong Xu, Yutong Ban, Guillaume Delorme, Chuang Gan, Daniela Rus, and Xavier Alameda-Pineda. 2021. Transcenter: Transformers with dense queries for multiple-object tracking. *arXiv e-prints* (2021), arXiv–2103.
 - [81] Fan Yang, Xin Chang, Sakriani Sakti, Yang Wu, and Satoshi Nakamura. 2021. ReMOT: A model-agnostic refinement for multiple object tracking. *Image and Vision Computing* 106 (2021), 104091.
 - [82] Fan Yang, Wongun Choi, and Yuanqing Lin. 2016. Exploit all the layers: Fast and accurate cnn object detector with scale dependent pooling and cascaded rejection classifiers. In *Proceedings of the IEEE conference on computer vision and pattern recognition*. 2129–2137.
 - [83] Fan Yang, Shigeyuki Odashima, Shoichi Masui, and Shan Jiang. 2023. Hard to Track Objects with Irregular Motions and Similar Appearances? Make It Easier by Buffering the Matching Space. In *Proceedings of the IEEE/CVF Winter Conference on Applications of Computer Vision*. 4799–4808.
 - [84] En Yu, Zhuoling Li, Shoudong Han, and Hongwei Wang. 2022. Relationtrack: Relation-aware multiple object tracking with decoupled representation. *IEEE Transactions on Multimedia* (2022).
 - [85] Haiyang Yu, Jingye Chen, Bin Li, Jianqi Ma, Mengnan Guan, Xixi Xu, Xiaoxiong Wang, Shaobo Qu, and Xiangyang Xue. 2021. Benchmarking chinese text recognition: Datasets, baselines, and an empirical study. *arXiv preprint arXiv:2112.15093* (2021).
 - [86] Haiyang Yu, Jingye Chen, Bin Li, and Xiangyang Xue. 2022. Chinese Character Recognition with Radical-Structured Stroke Trees. *arXiv preprint arXiv:2211.13518* (2022).
 - [87] Fangoang Zeng, Bin Dong, Yuang Zhang, Tiancai Wang, Xiangyu Zhang, and Yichen Wei. 2022. Motr: End-to-end multiple-object tracking with transformer. In *Computer Vision—ECCV 2022: 17th European Conference, Tel Aviv, Israel, October 23–27, 2022, Proceedings, Part XXVII*. Springer, 659–675.
 - [88] Hao Zhang, Feng Li, Shilong Liu, Lei Zhang, Hang Su, Jun Zhu, Lionel M Ni, and Heung-Yeung Shum. 2022. Dino: Detr with improved denoising anchor boxes for end-to-end object detection. *arXiv preprint arXiv:2203.03605* (2022).
 - [89] Kaiduo Zhang, Muye Sun, Jianxin Sun, Binghao Zhao, Kunbo Zhang, Zhenan Sun, and Tieniu Tan. 2022. HumanDiffusion: a Coarse-to-Fine Alignment Diffusion Framework for Controllable Text-Driven Person Image Generation. *arXiv preprint arXiv:2211.06235* (2022).
 - [90] Shanshan Zhang, Rodrigo Benenson, and Bernt Schiele. 2017. Citypersons: A diverse dataset for pedestrian detection. In *Proceedings of the IEEE conference on computer vision and pattern recognition*. 3213–3221.
 - [91] Yang Zhang, Hao Sheng, Yubin Wu, Shuai Wang, Weifeng Lyu, Wei Ke, and Zhang Xiong. 2020. Long-term tracking with deep tracklet association. *IEEE Transactions on Image Processing* 29 (2020), 6694–6706.
 - [92] Yifu Zhang, Peize Sun, Yi Jiang, Dongdong Yu, Fucheng Weng, Zehuan Yuan, Ping Luo, Wenyu Liu, and Xinggang Wang. 2022. Bytetrack: Multi-object tracking by associating every detection box. In *Computer Vision—ECCV 2022: 17th European Conference, Tel Aviv, Israel, October 23–27, 2022, Proceedings, Part XXII*. Springer, 1–21.
 - [93] Yifu Zhang, Chunyu Wang, Xinggang Wang, Wenjun Zeng, and Wenyu Liu. 2021. Fairmot: On the fairness of detection and re-identification in multiple object tracking. *International Journal of Computer Vision* 129 (2021), 3069–3087.
 - [94] Yuang Zhang, Tiancai Wang, and Xiangyu Zhang. 2022. MOTRv2: Bootstrapping End-to-End Multi-Object Tracking by Pretrained Object Detectors. *arXiv preprint arXiv:2211.09791* (2022).
 - [95] Zelin Zhao, Ze Wu, Yueqing Zhuang, Boxun Li, and Jiaya Jia. 2022. Tracking objects as pixel-wise distributions. In *Computer Vision—ECCV 2022: 17th European Conference, Tel Aviv, Israel, October 23–27, 2022, Proceedings, Part XXII*. Springer, 76–94.
 - [96] Liang Zheng, Hengheng Zhang, Shaoyan Sun, Manmohan Chandraker, Yi Yang, and Qi Tian. 2017. Person re-identification in the wild. In *Proceedings of the*

- IEEE conference on computer vision and pattern recognition*. 1367–1376.
- [97] Xingyi Zhou, Vladlen Koltun, and Philipp Krähenbühl. 2020. Tracking objects as points. In *Computer Vision—ECCV 2020: 16th European Conference, Glasgow, UK, August 23–28, 2020, Proceedings, Part IV*. Springer, 474–490.
- [98] Xingyi Zhou, Dequan Wang, and Philipp Krähenbühl. 2019. Objects as points. *arXiv preprint arXiv:1904.07850* (2019).
- [99] Xingyi Zhou, Tianwei Yin, Vladlen Koltun, and Philipp Krähenbühl. 2022. Global tracking transformers. In *Proceedings of the IEEE/CVF Conference on Computer Vision and Pattern Recognition*. 8771–8780.
- [100] Jiawen Zhu, Simiao Lai, Xin Chen, Dong Wang, and Huchuan Lu. 2023. Visual Prompt Multi-Modal Tracking. *arXiv preprint arXiv:2303.10826* (2023).
- [101] Xizhou Zhu, Weijie Su, Lewei Lu, Bin Li, Xiaogang Wang, and Jifeng Dai. 2020. Deformable detr: Deformable transformers for end-to-end object detection. *arXiv preprint arXiv:2010.04159* (2020).

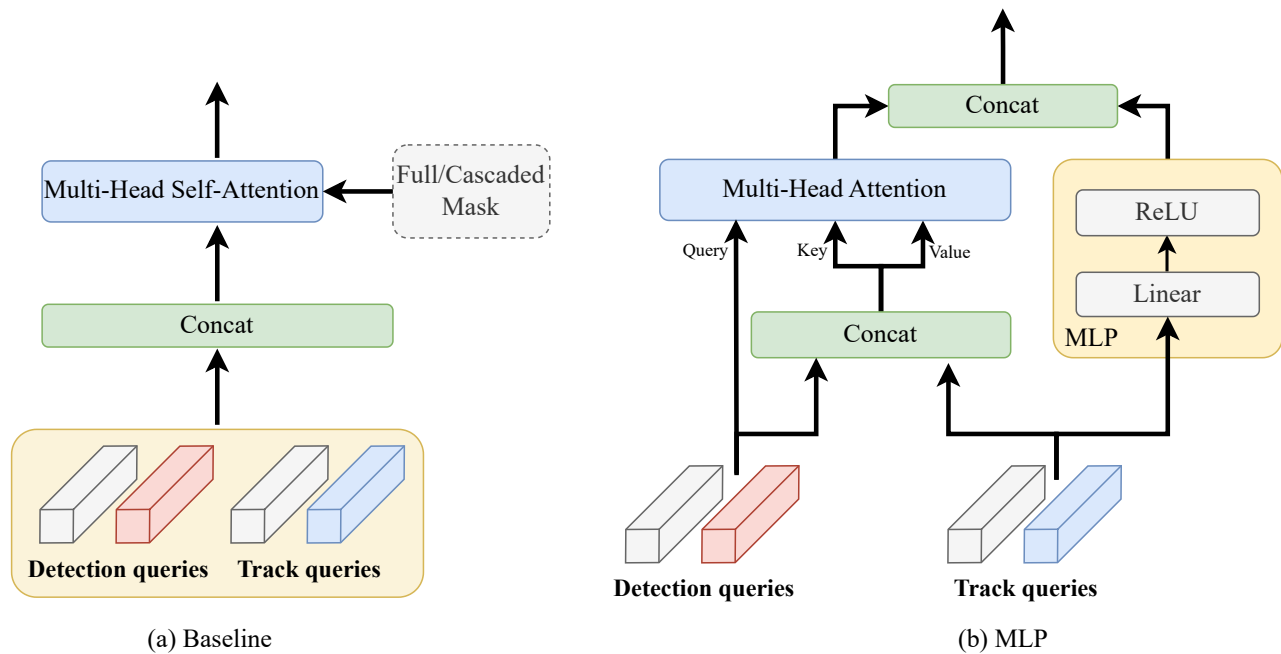


Figure 7: Network architecture in the ablation experiment of "Cascaded Mask" in the main text. (a) illustrates our baseline (without "Full/Cascaded Mask"), which is used in most Transformer-based models, and we add different masks innovatively. (b) illustrates the architecture of MLP we performed in the experiment. We utilize the same processing method for denoising queries across all experiments, so we omit it from the figure.

A DETAILS OF NETWORK ARCHITECTURE IN ABLATION EXPERIMENTS

In this section, we provide the details of the network architecture used in the ablation experiment of "Cascaded Mask" in Figure 7. We use the ablation experiment to explore the interaction between different types of queries. Because Denoising queries have the same processing method in all the experiments, we omit them in the figure.

In the previous methods [42, 87], as in Figure 7(a) (without Full/Cascaded Mask), different types of queries are concatenated and passed to Self-Attention module to interact with each other. Considering the track queries are invisible to each other, we design an MLP to replace the original Self-Attention module. To process detection queries, all the queries are concatenated like previous methods as Key and Value, while only detection queries are used as Query. On the other hand, for the track queries, we use a MLP network, which contains a linear layer and an activation function. Finally, track queries and detection queries are concatenated and passed to the next stage.

As indicated in Table 6 in the main text, we finally use the mask to coordinate the interaction between different types of queries (Figure 7(a) with Full/Cascaded Mask).

B ALGORITHM OF GENERATION OF DENOISING QUERIES

We provide the generation process of Denoising queries in Algorithm 1, as a more detailed description of Figure 4(b) in the main text.

C ANALYSIS OF DATASETS

In this section, we analyze the degree of crowdedness of the MOT17, MOT20 and DanceTrack dataset. To quantify this, we count the number of frames and pedestrians in training set of each dataset, and then we calculate the number of pairs with IOU scores greater than specific thresholds for each sequence. This allows us to obtain the average number of crowded pairs and pedestrians for each dataset, which characterizes their density levels.

For MOT17, our statistical results are demonstrated in Table 8. MOT17 contains **204,701** pedestrians spread across 5,316 frames, giving an average of **38** pedestrians per frame. Additionally, on average, there are only **2.5** pairs of pedestrians with an Intersection over Union (IOU) score greater than 0.4, indicating relatively low crowdedness in the dataset.

For MOT20, our statistical results are demonstrated in Table 9. MOT20 contains a total of **1,134,614** pedestrians distributed over 8,931 frames, yielding an average of **127** pedestrians per frame. On average, about **20** pairs of pedestrians have an IOU score greater than 0.4. So MOT20 is more crowded in both the average number of people per frame and the average number of crowded pairs, and our model's high

Algorithm 1: The generation process of denoising queries

Input: Bounding boxes in ground truth $B = \{B_1, B_2, \dots, B_N\}$;
Active trajectories $T = \{T_1, T_2, \dots, T_N\}$;
Correspondence between trajectories and ground truth M ;
Category perturbation range C , conditional noise threshold λ_c , conditional noise probability p ;
positive noise range λ_r , negative noise range λ_n ;
Output: N_g groups of denoising queries

- 1 Initialize group number of denoising queries: $N_g = 200 // B.length$
- 2 **for** $group = 1$ to N_g **do**
- 3 Randomly take $B.length$ category IDs from the range $[0, C]$ to form class set S_a ;
- 4 Map IDs in S_a to class embeddings;
- 5 Assign a bounding box in B to each class embedding;
- 6 Replace the corresponding class embedding with the tacklet embedding according to M ;
- 7 **for** each bounding box and class embedding pair **do**
- 8 Calculate the IOU scores between the bounding box and others;
- 9 **if** At least an IOU score greater than λ_c **then**
- 10 **if** Random number $\leq p$ **then**
- 11 Random select a bounding box which IOU score greater than λ_c ;
- 12 Generate a Noise position via Eq 2 in the main text;
- 13 **else**
- 14 Sample four noise factors $N = (n_x, n_y, n_w, n_h)$ from range $[-\lambda_r, \lambda_r]$;
- 15 Generate a Noise position via Eq 1 in the main text;
- 16 Add the result to positive set S_p ;
- 17 **else**
- 18 Sample four noise factors $N = (n_x, n_y, n_w, n_h)$ from range $[-\lambda_r, \lambda_r]$;
- 19 Generate a Noise position via Eq 1 in the main text;
- 20 Add the result to S_p ;
- 21 Sample four noise factors $N = (n_x, n_y, n_w, n_h)$ from range $[-\lambda_n, \lambda_n]$;
- 22 Generate a Noise position via Eq 1 in the main text; add the result to negative set S_n ;
- 23 **end**
- 24 Concatenate S_p and S_n as a group of denoising queries.
- 25 **end**

robustness to occlusion leads to a greater improvement on MOT20 (+1.9 in MOTA, +7.1 in IDF1 and +3.9 in HOTA) than on MOT17 (+1.5 in MOTA, -0.9 in IDF1 and +0.2 in HOTA).

For DanceTrack, our statistical results are demonstrated in Table 10. There are **348930** pedestrians in a total of 41796 frames, which means there are around **8** pedestrians in a frame on average, while there is around **1** pair of pedestrians can have a IOU score more than 0.4. Compared to MOT17, DanceTrack has a more sparse object distribution, but a similar number of crowded pairs. Moreover, the objects in DanceTrack have similar dress, which makes it more challenging to distinguish and track them. The significant improvement in performance (+2.0 in HOTA) achieved by our model on DanceTrack further validates its effectiveness in handling complex scenarios.

D COMPARISON WITH GENERATIVE MODELS

Generative model [21, 31, 52, 62] gets a lot of attention because of the appearance of diffusion model, and the excellent performance in applications like AIGC makes the study [53, 54] of this technology more and more popular. Like our method, the diffusion models also uses the concept of "noise and denoise". These methods gradually add Gaussian noises to the original image until the image becomes a totally noisy image, then a network is used to gradually denoise the image until the image becomes the original image.

There are several differences between our method and the generative model like diffusion model:

- **Purposes of noising.** Our purpose is to simulate the occurrence of occlusion by adding noises, while the diffusion model just adds noise to make the image gradually become pure Gaussian noise.
- **Format of noising.** Our noises are bounding boxes-level, while the noises of the diffusion model are pixel-level.
- **Procedures of denoise.** We use a decoder architecture directly regress the original bounding box or map the noising bounding boxes to the category of "no-object", while diffusion gradually restores the original image using the network repeatedly.

Table 8: Degree of crowdedness in train set of MOT17 dataset.

Sequence	0.1-0.4	0.4-0.5	0.5-0.6	0.6-0.7	0.7-0.8	0.8-0.9	>0.9
MOT17-02	9648	1113	1126	1104	545	187	7
MOT17-04	16696	2292	1387	1068	350	75	0
MOT17-05	2143	202	114	61	33	8	4
MOT17-09	2496	344	380	213	136	33	0
MOT17-10	3382	493	318	190	98	26	1
MOT17-11	2770	222	48	36	6	1	0
MOT17-13	3222	376	278	231	167	33	8
Overall	40357	5042	3651	2903	1302	367	20
Average per frame	7.5916	0.9484	0.6868	0.5461	0.2449	0.0690	0.0038

Table 9: Degree of crowdedness in train set of MOT20 dataset. MOT20 has more pedestrians and pairs that have an IOU score greater than 0.4.

Sequence	0.1-0.4	0.4-0.5	0.5-0.6	0.6-0.7	0.7-0.8	0.8-0.9	>0.9
MOT20-01	15706	2157	1476	704	254	53	0
MOT20-02	164874	19619	11632	6141	2695	909	94
MOT20-03	224287	15828	7300	2759	908	281	19
MOT20-05	669205	60809	31285	12185	2963	883	199
Overall	1074072	98413	51693	21789	6820	2126	312
Average per frame	128.0029	11.7284	6.1605	2.5967	0.8128	0.2537	0.0372

E COMPARISON WITH METHODS IN OTHER FIELDS WHICH ADOPT “NOISING-AND-DENOISING” STRATEGY

Compared to the generative model, there are also many discriminative models that follow the concept of “noise and denoise”. In this section, we compare the difference between our model and methods using denoising paradigm in other fields (e.g., DN-DETR [35] and DINO [88] in object detection, which is our baseline).

Though our method follows the negative noise and noise mask module proposed in those methods, we innovatively propose the cascaded mask and conditional noises according to the severe occlusions. Overall, the differences between our method and others are as follows:

- The generation of denoising queries in other methods is completely random, which lacks consideration for the surrounding environment, including objects of the same and different categories. In our method, we consider the complex environment around the tracking object, and according to whether there are other objects in the vicinity, propose innovative conditional noises, and simulate the ID switches occurred in the crowded scenes.
- We also use a Mask to coordinate different types of queries in decoder, but we mainly focus on track queries rather than denoising queries, because unlike other methods in other fields, the relationship among the track queries and the relationship between track queries and other queries is the key of MOT. Besides, we propose a Cascaded Mask Module to dynamically adapt our design of mask, so in different stages of decoder, the track queries can interact with each other and focus on themselves, respectively.
- Our method is the first to use the “noise and denoise” paradigm in the multiple object tracking.

F DETAILED EXPERIMENTAL SETUP

In Table 11, we provide our hyperparameters in our experiments. Learning rate is initialized as 2×10^{-4} and decays to 2×10^{-5} after 10 epochs. We pretrain with 80 epochs in CrowdHuman and then train 40, 50 and 20 epochs in MOT17 [43], MOT20 [19] and DanceTrack [65], respectively. The backbone is ResNet50 and we use 4 levels of feature map as mentioned in the main text. We adopt 6 layers of encoder layers and 6 layers of decoder layers while the hidden dimension is set to 288 and the number of head is set to 8. Because MOT20 has more objects than other datasets, we set the number of detection queries to 300 in MOT20 while 150 in others. We follow Deformable DETR and set the number of sampled points to 4 in both encoder and decoder. The total number of positive denoising queries is limited to 200 and we noise the calss ID up to 20. For the loss function, we set all the weight to 1 and among track loss, we set the weight of focal loss, L1 loss and IOU loss to 1.0, 5.0 and 2.0, respectively. The positive noises range factor is set to 0.2 and negative noises factor is set to 0.4, while in positive noises, if there exists condition positive noises, the probability is 0.6.

Table 10: Degree of crowdedness in train set of DanceTrack dataset. DanceTrack has a more sparse people distribution but similar number of crowded pairs. And people in DanceTrack have more similar dress.

Sequence	0.1-0.4	0.4-0.5	0.5-0.6	0.6-0.7	0.7-0.8	0.8-0.9	>0.9
dancetrack0001	1162	271	120	35	15	1	0
dancetrack0002	1938	218	196	162	47	7	0
dancetrack0006	4160	704	545	336	119	23	2
dancetrack0008	1901	271	231	155	116	32	1
dancetrack0012	8149	1343	894	475	199	37	3
dancetrack0015	5496	363	113	27	5	0	0
dancetrack0016	4394	581	248	102	36	1	0
dancetrack0020	19402	2506	1071	574	209	40	6
dancetrack0023	4295	878	682	355	124	38	2
dancetrack0024	1151	152	70	40	11	1	0
dancetrack0027	1816	276	186	107	73	41	4
dancetrack0029	3474	1088	385	86	8	0	0
dancetrack0032	1015	190	177	132	75	10	2
dancetrack0033	2819	530	339	209	170	29	3
dancetrack0037	3025	392	360	184	134	17	2
dancetrack0039	2115	195	103	42	4	1	0
dancetrack0044	6379	817	459	230	95	15	1
dancetrack0045	7271	1319	736	290	84	11	1
dancetrack0049	3937	786	462	227	116	32	2
dancetrack0051	6377	1247	816	328	69	11	0
dancetrack0052	1293	166	100	95	64	15	1
dancetrack0053	1147	159	92	53	22	1	0
dancetrack0055	1219	176	97	56	35	6	0
dancetrack0057	655	83	43	15	7	1	0
dancetrack0061	1392	102	61	41	25	5	0
dancetrack0062	1027	193	91	42	26	9	0
dancetrack0066	1328	187	136	72	28	3	1
dancetrack0068	2479	364	253	160	55	11	0
dancetrack0069	2574	247	97	26	9	0	0
dancetrack0072	1849	250	147	78	28	4	0
dancetrack0074	2566	307	115	31	3	0	0
dancetrack0075	1965	196	131	61	79	20	0
dancetrack0080	3793	220	62	3	2	0	0
dancetrack0082	6668	509	119	14	7	1	0
dancetrack0083	9673	528	105	13	1	0	0
dancetrack0086	8182	1112	531	184	51	0	0
dancetrack0096	10401	1644	880	179	15	1	0
dancetrack0098	4371	767	406	132	48	4	0
dancetrack0099	5676	664	291	106	32	16	0
Overall	164091	22717	12360	5603	2303	465	31
Average per frame	3.9260	0.5435	0.2957	0.1341	0.0551	0.0111	0.0007

G VISUALIZATION

In this section, we provide more [89] visualization results. For MOT17 and MOT20 dataset, we randomly display three consecutive frames for all sequences in test set in Figure 9 and Figure 10, respectively. For DanceTrack, there are 35 sequences in test set, so we select the first part of sequences and randomly display three consecutive frames for those sequences in Figure 8.

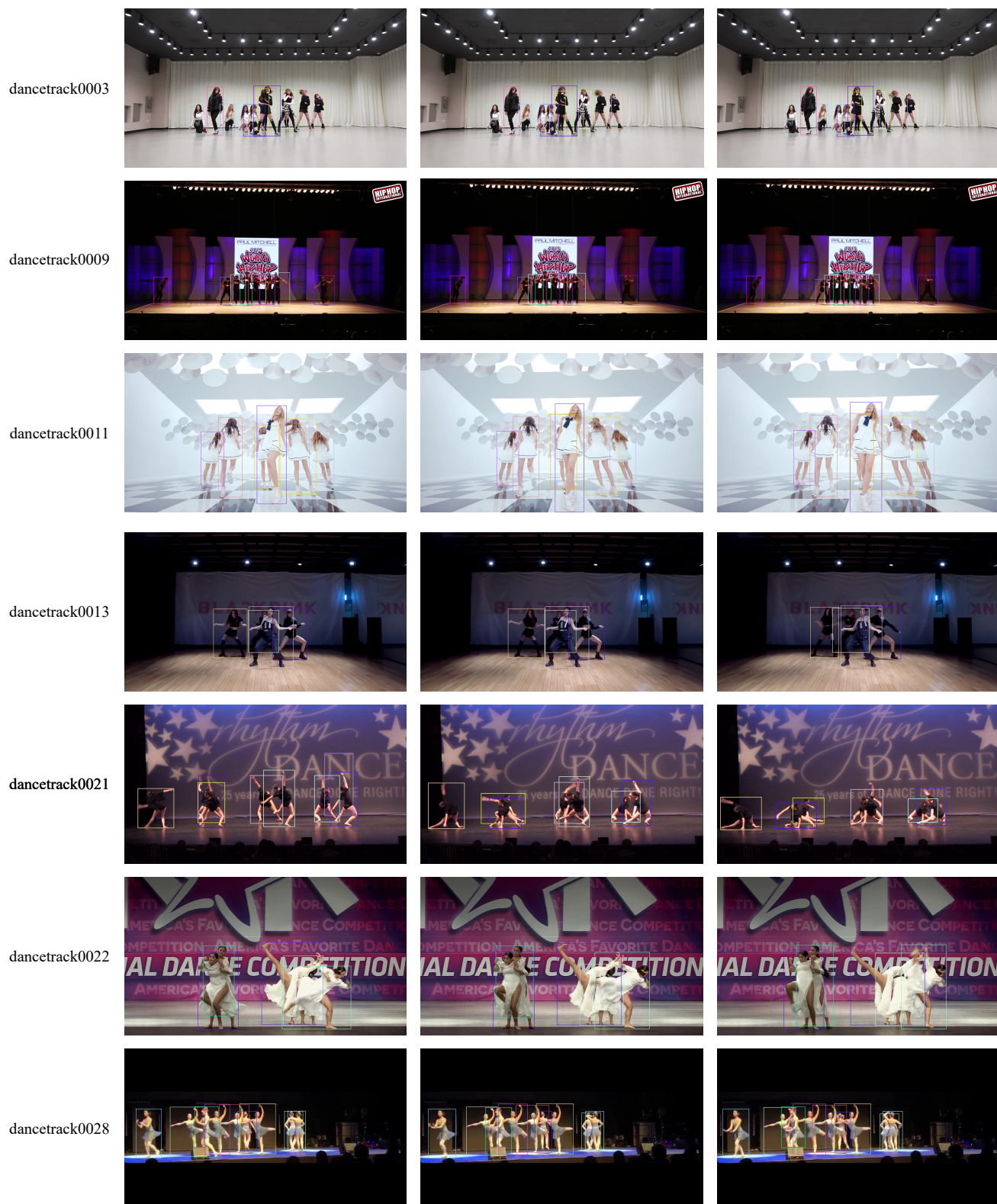


Figure 8: Visualization of sequences in DanceTrack test set.



Figure 9: Visualization of sequences in MOT17 test set.

Table 11: Hyperparameter settings in our experiments.

Parameter	MOT17	MOT20	DanceTrack
<i>Learning rate (Transformer)</i>	2×10^{-4}	2×10^{-4}	2×10^{-4}
<i>Learning rate (Backbone)</i>	2×10^{-5}	2×10^{-5}	2×10^{-5}
<i>Epoch</i>	40	50	20
<i>Learning rate decay epoch</i>	10	10	10
<i>Learning rate decay rate</i>	0.1	0.1	0.1
<i>Backbone</i>	ResNet50	ResNet50	ResNet50
<i>Number of feature levels</i>	4	4	4
<i>Number of encoder layers</i>	6	6	6
<i>Number of decoder layers</i>	6	6	6
<i>Hidden_dim</i>	288	288	288
<i>Dropout rate</i>	0.1	0.1	0.1
<i>Number of heads in Attention</i>	8	8	8
<i>Number of detection queries</i>	150	300	150
<i>Number of sampled points in encoder</i>	4	4	4
<i>Number of sampled points in decoder</i>	4	4	4
λ_{focal}	1.0	1.0	1.0
λ_{L1}	5.0	5.0	5.0
λ_{iou}	2.0	2.0	2.0
λ_{track}	1.0	1.0	1.0
λ_{aux}	1.0	1.0	1.0
λ_{inter}	1.0	1.0	1.0
λ_{r}	0.2	0.2	0.2
λ_{n}	0.4	0.4	0.4
λ_{c}	0.4	0.6	0.6
<i>Category noise range</i>	20	20	20
<i>Number of Denoising queries</i>	200	200	200

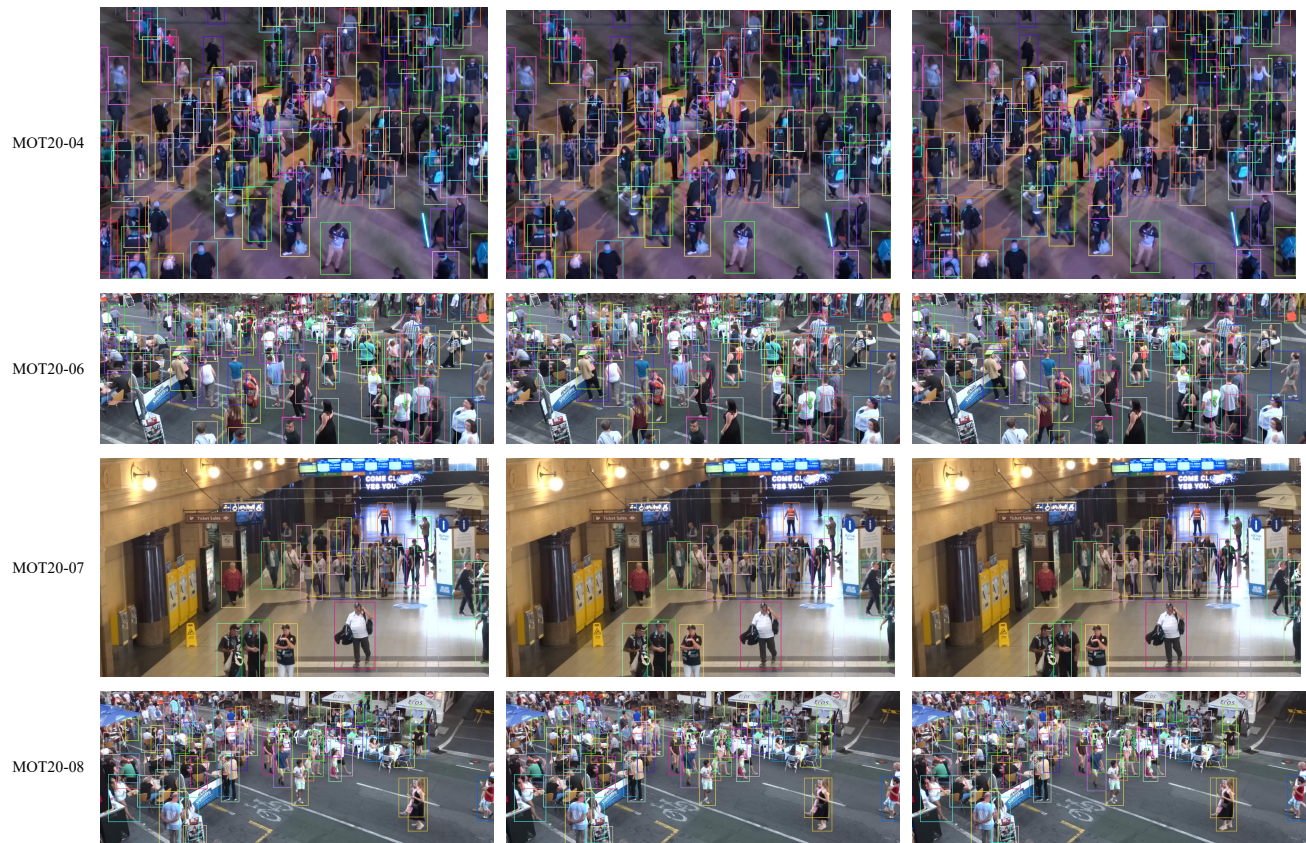


Figure 10: Visualization of sequences in MOT20 test set.